

# Induction of Apoptosis in MCF-7 Human Breast Cancer Cells by Phytochemicals from *Anoectochilus formosanus*

Lie-Fen Shyur<sup>a</sup> Chih-Huai Chen<sup>b,c</sup> Chiu-Ping Lo<sup>a</sup> Sheng-Yang Wang<sup>a</sup>  
Pei-Ling Kang<sup>a</sup> Show-Jane Sun<sup>a</sup> C. Allen Chang<sup>c</sup> Chi-Meng Tzeng<sup>b</sup>  
Ning-Sun Yang<sup>a</sup>

<sup>a</sup>Institute of BioAgricultural Sciences, Academia Sinica, and <sup>b</sup>Department of R & D, U-Vision Biotech Inc., Taipei, and <sup>c</sup>Department of Biological Science and Technology, National Chiao Tung University, Hsinchu, Taiwan, ROC

## Key Words

*Anoectochilus formosanus* Hayata (Orchidaceae) · Apoptosis · Fas ligand · Functional genomics · MCF-7 cells

## Abstract

The antitumor activity of *Anoectochilus formosanus* Hayata (Orchidaceae), a popularly used folk medicine in the treatment of cancers in Asia, was investigated in MCF-7 human mammary carcinoma cells. Plant extracts of *A. formosanus* were observed to induce apoptosis of MCF-7 cells as evidenced by cell-morphological changes, an early redistribution of plasma membrane phosphatidylserine, and DNA content distribution studies. Bioactivity-guided fractionation of *A. formosanus* extracts produced a specific ethyl acetate (EA)-partitioned fraction in which apoptotic activity was enriched. The chemical profile and candidate index compounds of the active EA fraction were obtained using HPLC and various spectral analyses. Western blot analysis showed that upon treatment of MCF-7 cells with the EA fraction, cleavage of pro-caspases-8, -9, and -7, and poly(ADP-

ribose) polymerase as well as significant release of mitochondrial cytochrome c into the cytosol were readily observed. Flow cytometry showed that the Fas ligand protein was overexpressed in EA-treated MCF-7 cells. Functional genomic studies indicated that specific genes related to cytoskeleton rearrangement, apoptotic signal transduction, and various transcription factors were differentially regulated in EA-treated MCF-7 cells. Putative apoptotic signaling pathways of MCF-7 cells in response to the EA extract of *A. formosanus* are proposed.

Copyright © 2004 National Science Council, ROC and S. Karger AG, Basel

## Introduction

Apoptosis, a form of programmed cell death, is either developmentally regulated or activated in response to specific extracellular and intracellular stimuli or cell injury [18]. In mammalian cells, apoptosis can be triggered by members of the Fas and TNF receptor families [14]. Recent studies have shown that apoptosis often involves disruption of mitochondrial membrane integrity, resulting in the release of cytochrome c from mitochondria into the cytosol, and this activity serves as a decisive factor for the onset of the cell death process [27]. A number of other cellular mechanisms are also known to be involved in the

Chih-Huai Chen and Chiu-Ping Lo contributed equally to this work.

## KARGER

Fax + 41 61 306 12 34  
E-Mail karger@karger.ch  
www.karger.com

© 2004 National Science Council, ROC  
S. Karger AG, Basel  
1021-7770/04/0116-0928\$21.00/0  
Accessible online at:  
www.karger.com/jbs

Lie-Fen Shyur  
Institute of BioAgricultural Sciences, Academia Sinica  
Nankang, Taipei 11529, Taiwan (ROC)  
Tel. +886 2 26515028, Fax +886 2 27899322  
E-Mail lfshyur@ccvax.sinica.edu.tw

process of apoptosis, including the regulation of biochemical activities of a family of aspartate-specific cysteine proteases, known as caspases. Activated caspases can specifically cleave cellular death substrates and cause biochemical and morphological changes leading to apoptosis [6].

Recent advances in understanding the modes of action of various anticancer agents indicate that regardless of the diverse chemical nature of anticancer drugs, most of them elicit apoptosis in test tumor cells [7, 25]. For example, taxol has been demonstrated to induce tumor cell apoptosis via a mitochondrial-dependent pathway [9]. Also, some potent chemopreventive agents, such as sulindac and other nonsteroidal anti-inflammatory drugs, induce apoptosis in colon tumors, leading to the prevention of cancer [21]. Therefore, the discovery and use of apoptosis-inducing molecules and the evaluation of their mechanisms of action should aid in the therapeutic manipulation of cancers and also help to understand the intracellular pathways of apoptosis in cancerous cells.

Extracts of *Anoectochilus formosanus* are commonly used in herbal therapies and drink supplements administered to patients with cancer in Asian countries. However, the pharmacological activities of this empirically used medicinal herb remain to be scientifically elucidated. Recently, we reported that plant extracts of *A. formosanus* exhibit strong antioxidant activities, indicating the potential for its development into a chemopreventive agent [24]. In this report, we observed that an enriched ethyl acetate (EA) fraction from the hot water extract of *A. formosanus* conferred significant antiproliferative effects and induced apoptosis in the human MCF-7 breast cancer cell line. A phytochemical profile of the EA-bioactive fraction was obtained using HPLC, IR, LC-mass, and one- and two-dimensional NMR analyses.

Rapid analysis of differential gene expression on a genome-wide scale became feasible with the development of DNA microarray technology [8]. This strategy offers a systematic approach to search for effective targets for drug discovery and diagnostics [4]. Results of human cDNA microarray analysis in this report revealed that a specific set of apoptosis-related genes in MCF-7 cells was highly responsive to treatment with the EA fraction of *A. formosanus*. Our findings indicate that the EA fraction of *A. formosanus* induces apoptosis in MCF-7 cells via a Fas ligand-mediated mechanism, in which the gene and protein expressions of cytochrome c are dramatically increased, and the apical and executive caspases (caspases-8, -9, and -7) are activated.

## Materials and Methods

### Chemicals

3-(4,5-Dimethylthiazol-2-yl)-2,5-diphenyl tetrazolium bromide, MTT, N'-bis(2-ethanesulfonic acid, PIPES, 3-[(3-cholamidopropyl)-dimethylammonio]-1-propane-sulfonate, CHAPS, N-(2-hydroxyethyl) piperazine-N'-(2-ethanesulfonic acid), HEPES, and plumbagin were purchased from Sigma (St. Louis, Mo., USA). Agarose was obtained from Bio-Rad (Hercules, Calif., USA), curcumin was from ACROS ORGANICS (Morris Plains, N.J., USA), and RPMI 1640 growth medium from GIBCO™ (Invitrogen, N.Y., USA). All other chemicals and solvents used in this study were of reagent or HPLC grade.

### Plant Materials

Fresh *A. formosanus* Hayata (Orchidaceae) plants in the flowering stage were purchased from a reputable Anoectochilus Cultural Station at Puli, Nantou County, central Taiwan, as officially recommended by Dr. Hsin-Sheng Tsay of the Taiwan Agricultural Research Institute, Taichung, Taiwan, ROC. The authenticity of these *A. formosanus* plants was validated by the specific morphological and anatomical features of the flowers [12]. Voucher specimens (No. 642008010) were deposited at the Herbarium, Institute of Botany, Academia Sinica, Taipei, Taiwan, ROC.

### Preparation and Fractionation of Plant Extracts

Fresh whole plants of *A. formosanus* (1 kg) were extracted twice, by boiling for 2 h with 3 volumes of distilled water. The total crude plant extract (AF-hot, ~49 g dry weight) was collected by centrifugation at 24,000 g for 20 min at 4 °C, and then lyophilized to dryness. A stepwise ethanol fractionation procedure, using 50, 75, and 87.5% (v/v) ethanol, respectively, was employed to obtain the subfractions AH-I, AH-II, AH-III, and AH-sup from the AF-hot crude extract. The AH-sup (19.3 g), i.e. the remaining soluble fraction of the AF-hot extract treated with 87.5% ethanol, was then further subjected to differential solvent partitioning using EA, followed by butanol (BuOH), to yield the EA (≈ 1.2 g), BuOH (≈ 3.4 g), and water (≈ 14.4 g) subfractions, respectively.

### Cell Culture

MCF-7 cells obtained from the American Type Culture Collection (ATCC, Manassas, Va., USA) were grown in RPMI 1640 medium supplemented with 10% fetal bovine serum, 100 U/ml penicillin, and 100 µg/ml streptomycin. In initial comparative studies, 10% fetal bovine serum was tested for substitution with serum replacement 2 (Sigma). H184B5F5/M10 (ATCC) cells, a non-cancerous human mammary epithelial cell line, were grown in 90% MEM (GIBCO™) and 10% fetal bovine serum as suggested by the instruction manual provided by ATCC. All experiments were carried out at 37 °C and 5% CO<sub>2</sub> on confluent cells in the medium.

### Cell Viability Assay

MCF-7 cells ( $5 \times 10^3$  to  $1 \times 10^4$ ) were incubated with or without test plant extracts in medium in 96-well plates for 1–3 days. Cell viability was assayed using the MTT colorimetric dye reduction method. Survival of MCF-7 cells after treatment with plant extracts was calculated using the following formula: viable cell number (%) =  $[\text{OD}_{570} (\text{treated cell culture}) / \text{OD}_{570} (\text{control, untreated cell culture})] \times 100$ . A <sup>3</sup>H-thymidine incorporation assay was also employed to determine the anti-cell proliferation activity in plant extracts of

*A. formosanus*, following the experimental protocol described by Seufferlein and Rozenfurt [18].

#### *Fluorescent Microscopy and Flow-Cytometric Analyses of Tumor Cells*

The ApoAlert Annexin V Apoptosis kit (Clontech, Palo Alto, Calif., USA) was used to analyze apoptotic activity in MCF-7 carcinoma cells. Test cells were treated for 24 h with the EA fraction (1 mg/ml) or the vehicle control (0.1% DMSO), washed with PBS buffer, resuspended in binding buffer, and then stained with Annexin V-EGFP and/or propidium iodide (PI) for 15 min in the dark. Treated cells ( $\sim 2 \times 10^5$ ) were cytospun at 800 rpm for 5 min and viewed using a Nikon (Melville, N.Y., USA) ECLIPSE E800 phase-contrast fluorescent microscope.

MCF-7 cells ( $1 \times 10^6$  cells), treated with or without plant extracts, were harvested and fixed with 1 ml ice-cold 70% ethanol at 4°C for 2 h. Total cellular DNA was stained for 30 min in the dark with 50 µg/ml of a PI solution containing 100 µg/ml RNase A in PBS buffer. The number of cells with a sub-G1 DNA content divided by the number of cells with the DNA content in the whole-cell cycle was taken as a measure of the percentage of the apoptotic cell population, using a Coulter EPICS XL flow cytometer (Beckman/Coulter, Durham, N.C., USA). Data were generated from samples with at least 10,000 cells per assay and analyzed with the DNA MultiCycle program (Beckman/Coulter).

#### *Western Blot Analysis*

MCF-7 cells ( $2 \times 10^6$ ) were washed with PBS once and lysed in 100 µl lysis buffer [20 mM PIPES (pH 7.0), 10 mM NaCl, 1 mM EDTA, 0.1% CHAPS, 10% sucrose, 10 mM DTT, 5 mM HEPES, 0.05% (v/v) Triton X-100, 1 mM MgCl<sub>2</sub>, 2.5 mM EGTA, and 0.44% (w/v) β-glycerol-phosphate] plus 2 µl protease inhibitor cocktail set III (Calbiochem, San Diego, Calif., USA) for 20 min on ice and extensively vortex mixed every 5 min. After centrifugation, the protein concentration in the supernatant was determined using a dye-binding assay (Bio-Rad). Protein samples (40 µg) were separated in a 5–20% gradient mini-SDS-polyacrylamide gel and transferred onto a PVDF membrane (Millipore, Bedford, Mass., USA). Membranes were first blocked with 3% (w/v) non-fat dry milk in TBS buffer (10 mM Tris, pH 7.5, and 100 mM NaCl) for 30 min and then incubated with specific primary antibodies at 4°C overnight with agitation. Mouse anti-glyceraldehyde-3-phosphate dehydrogenase (GA3PDH; Biogenesis, Kingston, N.H., USA), rabbit anti-NF-κB (Oncogene Research Products, Boston, Mass., USA), mouse anti-poly(ADP-ribose) polymerase (PARP; Transduction Laboratories, Lexington, Ky., USA), mouse anti-cytochrome c (PharMingen, San Diego, Calif., USA), mouse anti-procaspases-2, -7, and -9 (PharMingen), and rabbit anti-procaspase-8 (BD Research Products, San Diego, Calif., USA) antibodies were individually used as primary antibodies. After washing with TBST buffer (0.1% Tween 20 in TBS buffer), the blotting membrane was treated with alkaline-phosphatase-conjugated secondary antibodies at room temperature for 2 h. Immunoreactive proteins were visualized by the enhanced chemiluminescence system according to the manufacturer's protocol (Amersham Pharmacia Biotech, Amersham Place, UK).

#### *mRNA Preparation and cDNA Probe Generation*

Total cellular RNA samples of MCF-7 cells treated with plant extracts or vehicle control (0.4% DMSO) for 3, 6, 9, 12, 18, and 24 h were prepared using the Trizol<sup>®</sup> reagent and further purified using

the RNeasy<sup>®</sup> kit (QIAGEN, Cologne, Germany). Biotin-labeled cDNA probes were generated using the RT-PCR method described by Lau et al. [11].

#### *Generation, Hybridization, and Colorimetric Signal Detection of a cDNA Microarray*

Candidate cDNAs for generating cDNA microarrays were prepared from IMAGE consortium gene pools or self-constructed cDNA clones using PCR. The PCR reaction mixtures (100 µl) consisted of 10 U Taq polymerase (Merck, Darmstadt, Germany), 0.2 µM of the desired primers, 200 µM dNTPs, and 10 ng of template DNA. PCR was performed with a thermocycling program of 3 min at 95°C, followed by 40 cycles of 1 min at 94°C, 1 min at 50°C, and 2 min at 72°C on a PrimusHT thermocycler (MWG-Biotech, High Point, N.C., USA). The PCR products were then precipitated by 70% EtOH (Merck, Darmstadt, Germany), vacuum dried, and dissolved in sterilized water to a final concentration of 1.1 µg/µl DNA ( $\approx 10^8$  molecules of DNA/spot), before being spotted onto a nylon membrane. Conversion of coordinate and database constructions was established using GeneTrend<sup>™</sup> software (U-Vision, Taipei, Taiwan, ROC). Probe hybridization and color development were adapted from the colorimetric system published elsewhere [11]. The PA5500<sup>™</sup> arrayer and nanoliter quantitative aspirate-dispenser (nQUAD<sup>™</sup>) with microplate stacker Pegasys<sup>™</sup> 150 (Cartesian Technologies, Research Triangle Park, N.C., USA) were the printing system for generating the DNA microarrays. A 3,000-dpi light scanner (Umax, Taipei, Taiwan, ROC) combined with Imagen<sup>®</sup> (Biodiscovery, Boston, Mass., USA) and QuantArray<sup>®</sup> software, and statistical programs developed at U-Vision Biotech, Taipei, Taiwan, ROC (<http://www.u-vision-biotech.com/>) were used to perform image and microarray data analyses.

#### *Chemical Fingerprint Analysis of the EA Fraction of A. formosanus*

Analytical HPLC was performed to analyze the chemical fingerprint of the EA fraction from the *A. formosanus* extract. A Waters (Milford, Mass., USA) HPLC system equipped with a Waters 600 controller, Waters delta 600 pump, and 2487 dual λ absorbance detector was used. A 5-µm Si-60 column (250 × 10 mm, Merck) was employed with two solvent systems: n-hexane (A) and ethyl acetate (B). The elution gradient profile was set as follows: 0–5 min, 70% A to B (isocratic); 5–15 min, 70–30% A to B (linear gradient); 15–20 min 30% A to B (isocratic), and 20–30 min 30–0% A to B, while the flow rate was set at 1.5 ml/min and the detector wavelength was set to 254 nm. Six pure compounds (1–6) eluted with retention times of 6.0 (1), 8.9 (2), 9.7 (3), 13.5 (4), 14.6 (5), and 18.0 (6) min, respectively, were collected for structural determination using various spectroscopic analyses. UV spectra of candidate index compounds were recorded with a Jasco V-550 spectrometer and IR spectra obtained from a Bio-Rad FTS-40 spectrophotometer. Electron-impact mass spectrometric (EIMS) and high-resolution EIMS data were collected with a Finnigan (Dreieich, Germany) MAT-958 mass spectrometer; NMR spectra were recorded with Bruker Avance (Bremen, Germany) 500 and 300 MHz FT-NMR spectrometers at 500 (<sup>1</sup>H) and 75 MHz (<sup>13</sup>C). Profiling and quantification of index compounds in the EA fraction were performed by HPLC. The peak areas corresponding to the contents of candidate index compounds in the chromatogram of a known concentration of the EA fraction were calculated based on a standard calibration curve of individual index compounds. Standard calibration curves (peak areas vs. concentrations) of compounds 2 and 4, ranging from 0.05 to 1 mg/ml, were first determined at OD<sub>254</sub>.

## Results

### *Cytotoxic Effects of A. formosanus Extracts on MCF-7 Cells*

The cytotoxic effects of plant extracts from *A. formosanus* on the viability of MCF-7 cells were determined by MTT assays. In setting up the test system, we observed a very similar pattern of cytotoxic effects for the total crude extract of the plant (AF-hot), regardless of whether the culture medium was supplemented with fetal bovine serum or serum substitute (data not shown), suggesting that components of fetal bovine serum did not affect the inhibition of MCF-7 cell proliferation conferred by the phytochemicals in *A. formosanus* extracts. We then observed that the AH-sup fraction showed the most significant cytotoxic effect on MCF-7 cells relative to the AF-hot, AH-I, AH-II, and AH-III fractions (data not shown). Less than 45% of tested cells were detected as being viable after treatment with 1.5 mg/ml AH-sup for 48 h. In contrast, more than 70% cell viability was observed in MCF-7 cells treated with AF-hot, AH-I, AH-II, or AH-III using the same dosage. The AH-sup fraction was therefore further fractionated using EA and butanol partitions to obtain more enriched and more potent sub-fractions. As shown in figure 1, the EA fraction conferred the greatest cytotoxicity to MCF-7 cells, as compared to the AF-hot, AH-sup, BuOH, and water sub-fractions. Dosages of plant extract/fraction required to inhibit 50% of MCF-7 cell proliferation ( $IC_{50}$ ) were found to be 0.86 mg/ml for AH-sup, 0.08 mg/ml for EA, 1.5 mg/ml for BuOH, and 2.7 mg/ml for the water fraction. Therefore, a 10-fold lower  $IC_{50}$  value for anti-MCF-7 cell proliferation was detected for the EA fraction as compared to that of AH-sup. Similar results were obtained from the  $^3H$ -thymidine incorporation assays (data not shown). These results strongly suggest that the cytotoxic effect of the *A. formosanus* extract on MCF-7 cells was effectively enriched in the EA fraction. We obtained very similar cytotoxicity results of EA fractions from different batch preparations (data not shown). In this study, two well-known phytochemicals, namely curcumin and plumbagin, were employed as positive controls in the anti-MCF-7 cell proliferation assays, with data also shown in figure 1. Curcumin has been reported to be involved in anti-cell proliferation and induction of apoptosis in various types of tumor cells including MCF-7 cells [23] and human renal carcinoma Caki cells [26]. Plumbagin, a single-compound drug isolated from *Plumbago rosea*, is a known plant naphthoquinone with demonstrated antitumor and antibacterial properties [10].  $IC_{50}$  values for anti-MCF-7 cell prolifera-

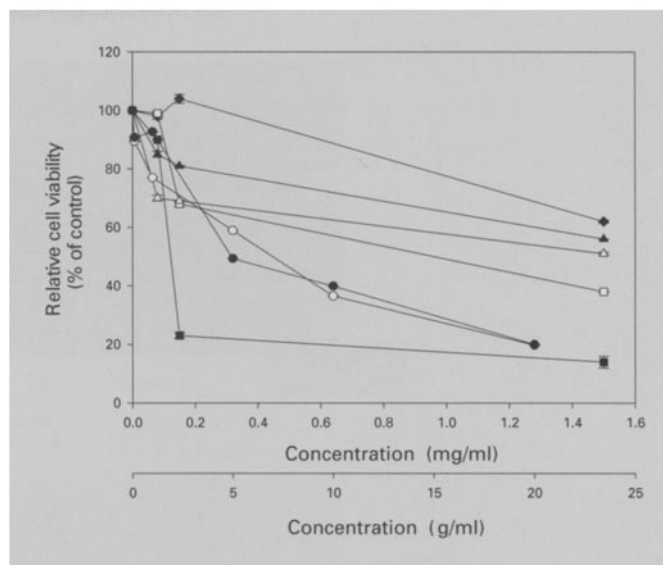


**Fig. 1.** Antiproliferative effect of AF-hot (◆), AH-sup (□), EA (■), BuOH (△), and water (▲) fractions of *A. formosanus* extract on MCF-7 mammary carcinoma cells. Relative cell viability (%) was measured 48 h after treatment of test cells with or without (control) the indicated doses of plant extracts (0.075–1.5 mg/ml) or curcumin (1–20  $\mu$ g/ml, ○), using MTT assays. Cell viability of plumbagin-treated MCF-7 cells (●) was determined after 3 h of treatment at doses ranging from 0.1 to 20  $\mu$ g/ml. Curcumin and plumbagin were used as positive controls in this experiment. Each data point represents the mean  $\pm$  SE of 3 independent experiments.

tion of curcumin and plumbagin were found to be 7.5  $\mu$ g/ml (48-hour treatment) and 5  $\mu$ g/ml (3-hour treatment), respectively.

H184B5F5/M10 cells, a non-cancerous human mammary epithelial cell line, were employed to test the potential cytotoxicity of the EA extract and curcumin using the MTT assay. We observed that the EA fraction exhibited an approximately 15-fold higher  $IC_{50}$  value ( $\sim$ 1,200  $\mu$ g/ml) for the antiproliferative effect against H184B5F5/M10 cells than that for anti-MCF-7 cell proliferation (80  $\mu$ g/ml) after 48 h of treatment. The  $IC_{50}$  values of curcumin for anti-MCF-7 and anti-H184B5F5/M10 cell proliferation were both determined to be approximately 7.5  $\mu$ g/ml after 48 h of treatment. These results indicate that curcumin conferred a lower specificity for discriminating between tumor and normal cell types as compared to that of the EA fraction of *A. formosanus*.

### *The EA Fraction of A. formosanus Extract Induces Apoptosis in MCF-7 Cells*

Light microscopy was employed to examine the cellular morphology of MCF-7 cells after treatment with *A. for-*

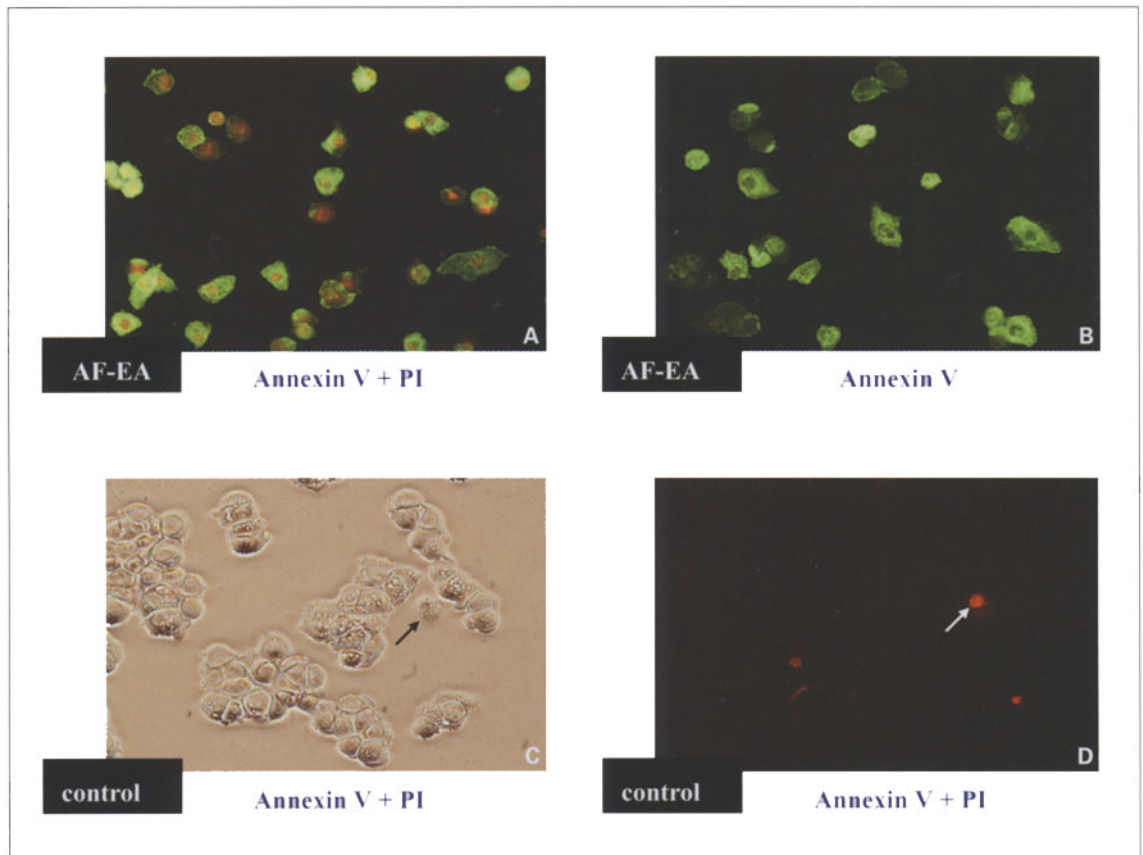


**Fig. 2.** Microscopic examination of normal versus EA fraction-treated MCF-7 cells in culture, as stained with Annexin-V and PI. log phase MCF-7 cells in culture were treated with the EA fraction (1 mg/ml) for 24 h and stained with PI plus Annexin-V (**A**) or Annexin-V alone (**B**). **C, D** MCF-7 cells treated with 0.1% DMSO (vehicle control), and stained with PI plus Annexin-V. **A, B, D** Fluorescent photomicrographs taken with an Olympus PM-30 camera on a Nikon ECLIPSE E800 microscope (magnification:  $\times 200$ ) using a B-2A filter (Ex 450–490). **C** Bright-field view of **D**.

*mosanus* extracts. In comparison to vehicle control-treated cells, EA-treated MCF-7 cells showed cell shrinkage, cytoplasmic blebbing, and the formation of apoptotic bodies (data not shown). An early redistribution of plasma membrane phosphatidylserine was also readily detected in MCF-7 cells after treatment with the EA fraction (1 mg/ml) for 24 h, as determined using Annexin V-GFP and PI staining (fig. 2), suggesting that the EA fraction effectively induced apoptosis in MCF-7 cells. We further used Annexin V-GFP staining (Clontech Laboratories) and flow cytometric analysis to examine the early events of apoptosis in MCF-7 cells induced by the EA fraction. We observed that the population of Annexin-V-stained MCF-7 cells increased in a dose-dependent manner when treated with the EA fraction for 24 h at concentrations ranging from 50 to 1,000  $\mu\text{g/ml}$ . Percentages of apoptotic

MCF-7 cells were determined to be 1.2, 2.9, 7, and 20% when test cells were treated with 50, 150, 500, and 1,000  $\mu\text{g/ml}$  EA, respectively. Figure 3 shows the typical flow cytometric profiles of DNA content and cell cycle behavior of MCF-7 cells with or without treatment with the EA extract. After 48 h of treatment, approximately 25% of total MCF-7 cellular DNA was detected as apoptotic (determined from the sub-G1 peak), and the level rose to 71% 72 h after treatment. Cell cycle arrest activity was not detected in MCF-7 cells treated with the EA fraction.

#### *The EA Extract Induces FasL Expression in MCF-7 Cells*

It is known that expression of the Fas ligand (FasL) can effectively mediate apoptosis by its binding to the cognate receptor, Fas [14]. In this study, results obtained from

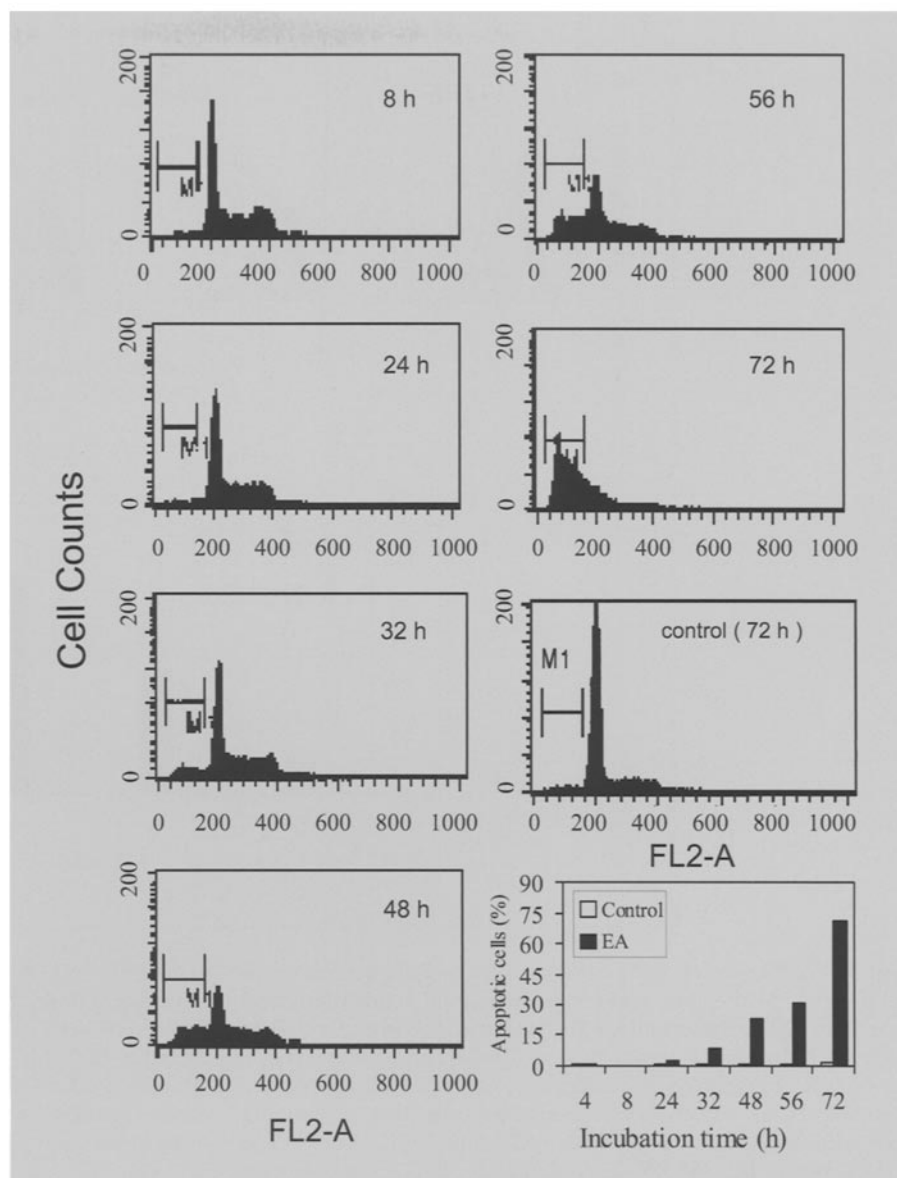


**Fig. 3.** Flow cytometric analysis of DNA content in normal and apoptotic MCF-7 cells, examined as a function of treatment time with the EA extract. MCF-7 cells were treated with either 0.4% DMSO (vehicle control) or 1 mg/ml of the EA fraction of *A. formosanus* extract, and later harvested at the indicated time points. M1 denotes the apoptotic peak.

flow cytometric analysis using the FITC-labeled anti-human FasL IgG1 antibody demonstrated that the EA extract of *A. formosanus* significantly induced the expression of FasL in MCF-7 cells. Upon treatment with EA for 5–16 h, FasL protein expression in MCF-7 cells drastically increased from 10 to 76%, relative to non-treated cells (fig. 4A, B), in a time-dependent manner. The TNF- $\alpha$ - and IFN- $\gamma$ -induced cell surface expressions of FasL in MCF-7 cells [15] were employed as reference controls in this experiment. Eighty percent FasL protein expression was observed in MCF-7 cells treated with both cytokines (fig. 4A, B).

#### *Cellular Mechanisms of EA-Fraction-Induced Apoptosis in MCF-7 Cells*

The potential cellular mechanisms of apoptosis in MCF-7 cells induced by the EA plant extract of *A. formosanus* were characterized using immunoblot analysis. Figure 5 shows that significant increases in the levels of cytosolic cytochrome c and proteolytic cleavage of pro-caspase-8 (~55 kDa) were detected within 16 h of MCF-7 cells being treated with the EA fraction (fig. 5A). Between 24 and 32 h after treatment, proteolytic processing of caspase-7 and -9, known to be involved in the early activation cascade of apoptosis, was also effectively activated in

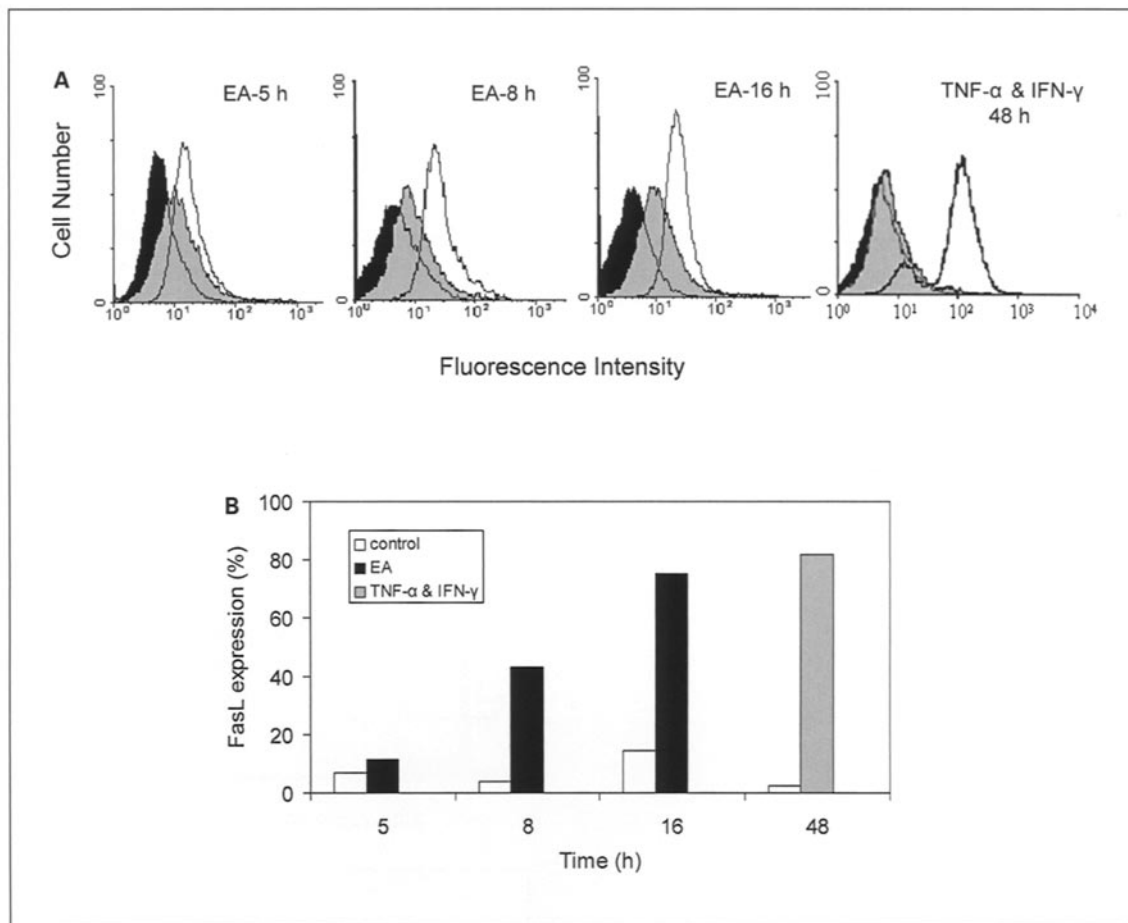


**Fig. 4.** EA fraction of *A. formosanus* induces FasL expression in MCF-7 cells. MCF-7 cells were untreated (isotype control) or treated with 1 mg/ml EA extract or 0.4% DMSO (vehicle control), for 5, 8, or 16 h. MCF-7 cells treated with 10 ng/ml TNF- $\alpha$  and 200 U/ml IFN- $\gamma$  for 48 h were employed as a reference control of FasL expression. FasL expression was quantified using flow cytometry, by staining cells with mouse anti-human FasL IgG (clone NOK-1) or isotype control mouse IgG (MOPC-21), followed by FITC-conjugated rat

anti-mouse IgG. **A** Fluorescent intensities obtained from isotype control cells (black images), vehicle control cells (gray images), and EA- or TNF- $\alpha$ +IFN- $\gamma$ -treated cells (white images), as analyzed using a Coulter EPICS XL flow cytometer (Beckman Coulter) with Expo XL 4 Cytometer software. **B** FasL protein expression (%) of vehicle control cells (white bars) and EA- (black bars) or TNF- $\alpha$ +IFN- $\gamma$ -treated cells (grey bar), relative to isotype control cells.

MCF-7 cells. Upon EA treatment, the level of Rel A, a subunit (p65) of NF- $\kappa$ B known to be directly involved in the inhibition of apoptosis [13], was only slightly suppressed in MCF-7 cells (fig. 5A). Time-dependent proteolytic cleavage of PARP, another hallmark of apoptosis, was observed with an accumulation of a 28-kDa product and a concomitant disappearance of the full-size, 113-kDa enzyme molecule (fig. 5B). Bcl-2 and Bax proteins in MCF-7 cells were not found to be responsive to EA treatment (data not shown).

#### *Gene Expression Profiles in MCF-7 Cells in Response to EA Treatment*

Broad-range, 9,800-dot, duplicate spot-formatted sets of known human cDNA microarrays were employed to collect genomic information on the mechanisms of *A. formosanus* extract-induced apoptosis in MCF-7 cells. Results from two duplicate experiments showed that the scatter plots derived from normalized signals at various treatment time points with EA were well correlated and reproducible. Along with statistical analysis of the annotation of specific genes and gene clusters, a summary of differentially expressed genes with at least 3-fold changes in

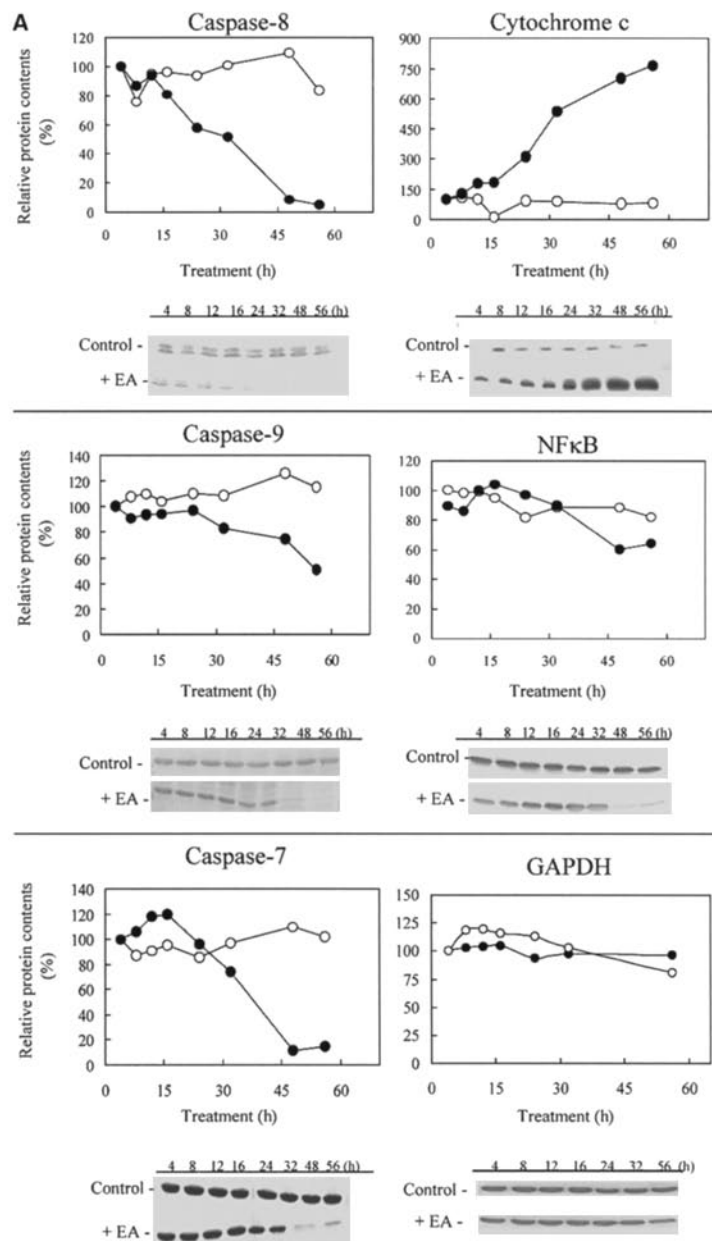


**Fig. 5.** Western blot analyses of caspases-7, -8, and -9, cytochrome c, NF- $\kappa$ B, GAPDH (A), and PARP (B) in MCF-7 cells treated with 0.4% DMSO (vehicle control) or with the EA fraction of *A. formosanus*. Aliquots of cell lysates were subjected to 5–20% SDS gradient gel electrophoresis. Detailed trans-blotting and immunostaining procedures are described in the Materials and Methods. Specific protein contents in control or EA-treated MCF-7 cells were quantified using densitometry. Relative protein contents (%) of EA-treated and control cells are presented as the protein level detected at various time points divided by the protein content at 4 h in either EA-treated or control cells.

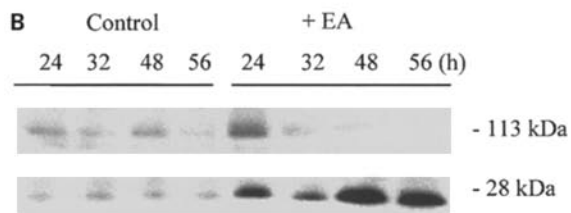




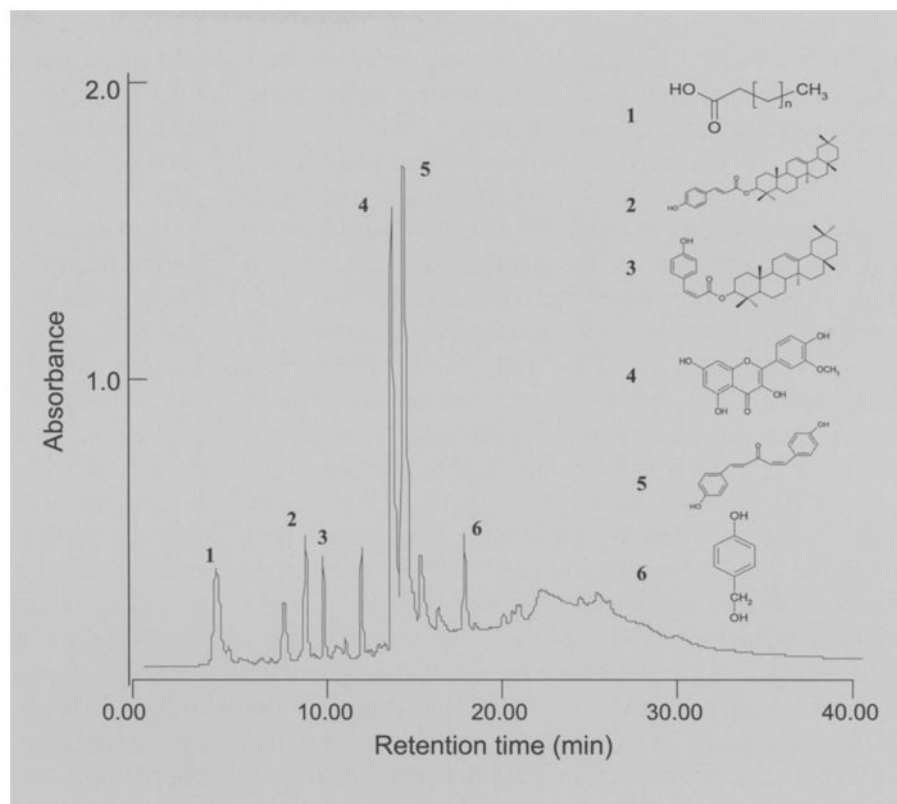
**Table 1.** Overview of differentially expressed genes in MCF-7 cells responsive to the EA fraction of *A. formosanus* revealed by DNA microarray and bioinformatic analyses

Genes	x-fold change
<b>Apoptosis</b>	
c-Jun proto-oncogene (JUN)	11
14-3-3 epsilon	5
Cytochrome c	5
ADP-ribosyltransferase (NAD <sup>+</sup> ; PARP)	5
Protein kinase C <sup>a</sup>	4
FAST	3
<b>Cell proliferation and growth arrest</b>	
Cyclin-dependent kinase inhibitor 2A	17
Protein phosphatase 2, regulatory subunit B (B56), $\gamma$ isoform <sup>a</sup>	12
DNJ3/CPR3 mRNA	10
Regulator of mitotic spindle assembly 1	9
<b>Cytoskeleton</b>	
<i>Group-specific component (vitamin D binding protein)</i>	4
<i>Cell division cycle 42 (GTP binding protein, 25 kDa): CDC42</i>	3
<i>Actin-related protein 2/3 complex, subunit 2, 34 kDa: ARPC2</i>	3
<b>Signal transduction</b>	
Protein phosphatase 2, regulatory subunit B (B56), $\gamma$ isoform <sup>a</sup>	12
Phosphotyrosine-independent ligand p62 for the Lck SH2	10
Tight junction protein 1 (zona occludens 1)	10
Tyrosine kinase (Tnk1)	6
Galactokinase 1	6
Diacylglycerol kinase $\delta$	5
Protein tyrosine phosphatase, non-receptor type 12	5
ATP synthase lipid-binding protein P2 precursor	5
Phosphatidylinositol 4-kinase $\alpha$ (PI4K- $\alpha$ )	5
Protein kinase C <sup>a</sup>	4
Phospholipase C $\delta$ 1	3
Type 1 inositol 1,4,5-trisphosphate receptor (IP3R-1)	3
Stress-activated protein kinase JNK2 <sup>a</sup>	3
<i>Stress-responsive serine/threonine protein kinase Krs-1<sup>a</sup></i>	5
<i>Protein tyrosine phosphatase, receptor type, c polypeptide</i>	3
Genes denoted in italics represent those that were downregulated in MCF-7 cells.	
<sup>a</sup> Genes that can be subgrouped into more than 1 functional category.	

MCF-7 cells is shown in table 1. In total, 52 genes of MCF-7 cells were found to exhibit more than a 3-fold change in specific activity when treated with the EA fraction, and 28 of them functionally relevant to apoptosis and signal transduction are listed in table 1. For example, the mRNA expression levels of cytochrome c, PARP, and TGF- $\beta$  superfamily proteins were upregulated, correlating well with the observed activity of apoptosis in test cells. Gene expressions of caspases-2 and -8, however, were not found to be responsive to EA treatment. It has been demonstrated that activation of caspase-8 occurs through autoproteolytic processing after formation of pro-

caspase-8 protein oligomers, leading to the initiation of the caspase signaling cascade in apoptotic cells [5, 17, 29]. Our observations agree well with and are supported by the model in which the autoprocessing of caspase-8, without affecting its transcription level, initiates the proteolysis of the downstream executive caspases, e.g. caspase-7 in our case. The cell division cycle 42 (*cdc42*) gene was found to be downregulated after 9 h of EA treatment. More than a 5-fold increase in gene expression levels were detected for the regulator of mitotic spindle assembly 1, diacylglycerol kinase  $\delta$ , and c-Jun proteins, which were demonstrated to be correlated to morphological changes in apoptotic cells,

**Fig. 6.** Chemical fingerprints and candidate index compounds of the EA fraction of *A. formosanus*. The chromatogram of the EA fraction was obtained from a Si-60 HPLC system. Six compounds are suggested in this study as useful index or reference compounds, including (1) a long-chain aliphatic acid; (2)  $\alpha$ -amyirin *trans-p*-hydroxy cinamate; (3)  $\alpha$ -amyirin *cis-p*-hydroxy cinamate; (4) isorhamnetin; (5) kinsenoside, and (6) *p*-hydroxybenzyl alcohol.



as we suggested here for EA-treated MCF-7 cells. Fas-activated serine/threonine kinase (FAST) has been shown to be activated during Fas-mediated apoptosis [22]. In our experiments, a 3-fold increase in FAST gene expression, as evaluated using the cDNA microarray as well as Northern blot analyses, was observed in EA-treated MCF-7 cells (with 9 h of treatment).

#### Chemical Fingerprinting of the EA Fraction from *A. formosanus*

Mass spectrometric and NMR analyses together with spectral data published from our laboratory and others [1, 24] have led to the identification of six compounds in the EA fraction of *A. formosanus*. These include a long-chain aliphatic acid (1),  $\alpha$ -amyirin *trans-p*-hydroxy cinamate (2),  $\alpha$ -amyirin *cis-p*-hydroxy cinamate (3), isorhamnetin (4), kinsenoside (5), and *p*-hydroxybenzyl alcohol (6), as indicated by HPLC in figure 6. In this study,  $\alpha$ -amyirin *trans-p*-hydroxy cinamate (2) and isorhamnetin (4) were chosen as candidate index compounds of *A. formosanus*, and their contents were quantitatively determined in the bioactive EA fraction using HPLC. One gram of EA extract was quantitatively detected to contain 4.9 (0.49%)

and 52.3 mg (5.23%) of  $\alpha$ -amyirin *trans-p*-hydroxy cinamate and isorhamnetin, respectively. The spectral data of  $\alpha$ -amyirin *trans-p*-hydroxy cinamate and isorhamnetin are summarized as follows.

$\alpha$ -Amyirin *trans-p*-hydroxy cinamate (2): white solid; mp 105–106°C; EIMS for  $C_{29}H_{56}O_3$  found 572.43;  $^1H$ NMR ( $CDCl_3$ ):  $\sigma$  (ppm) 7.62 (d,  $J = 8.0$ ), 7.45 (d,  $J = 8.0$ ), 6.85 (d,  $J = 18.2$ ), 6.32 (d,  $J = 18.2$ ), 5.22 (m), 4.70 (m), 1.17 (s), 1.01 (s), 1.00 (s), 0.96 (s), 0.90 (s), 0.89 (s), 0.86 (s).

Isorhamnetin (4): yellow amorphous powder; EIMS for  $C_{16}H_{12}O_7$  found 312.6;  $^1H$ NMR ( $CDCl_3$ ):  $\sigma$  (ppm) 7.96 (d,  $J = 2.0$ ), 7.56 (d,  $J = 8.0, 2.1$ ), 7.04 (d,  $J = 7.8$ ), 6.39 (d,  $J = 2.0$ ), 6.20 (d,  $J = 2.0$ ).

#### Discussion

In the present study, we demonstrate that the EA extract of *A. formosanus* inhibits proliferation of MCF-7 human mammary carcinoma cells through the induction of cell apoptosis. Cellular, biochemical, and functional genomic evidences indicate that treatment with the *A. for-*

*mosanus* extract may have caused transcriptional disorder of cytoskeletal biosynthesis, accompanied by both FasL-induced proteolytic cell death and a protein-kinase-C-associated apoptotic process in MCF-7 cells.

FasL, a 40-kDa type II transmembrane protein, has previously been shown to mediate apoptosis by binding to its cognate receptor Fas (APO-1/CD95) [14], and FAST is activated during Fas-mediated apoptosis [22]. In this study, FasL protein levels were significantly increased and the mRNA expression level of FAST was upregulated upon EA treatment of MCF-7 cells (fig. 4, table 1). It is generally believed that there are two distinct primary apoptotic signaling pathways in mammalian systems: one mediated by death receptors controlled by caspases-8 and -10, and the other by release of cytochrome c and activation of a caspase-9/Apaf1/cytochrome c apoptosome [19]. We found that EA fraction-induced MCF-7 cell apoptosis occurred concomitantly with activation of caspase-8 (16 h after treatment), significant cytosolic cytochrome c accumulation (16–24 h after treatment), and the proteolytic digestion of caspase-9 (32 h after treatment; fig. 5). In this study, pro-caspase-7 was proteolytically cleaved in MCF-7 cells (24–32 h after EA treatment) after significant accumulation of cytochrome c in the cytosol (fig. 5). It has been reported that cytochrome c-triggered caspase activation can result in rapid cleavage of PARP [6]. In this study, the results of cDNA microarray, Northern blot, and Western blot analyses together demonstrated that in response to EA treatment, PARP was cleaved, and this cleavage, which was regulated at both the transcriptional and post-translational levels in MCF-7 cells, may have been due to the release of cytochrome c into the cytosol and activation of caspases. We, therefore, propose herein a putative apoptotic pathway (mechanism I) via FasL expression and activation of apical and executive caspases in MCF-7 cells upon treatment with the EA fraction of *A. formosanus*.

On the basis of the results obtained from functional genomic studies, we propose that another distinct apoptotic signaling pathway may be active in EA-treated MCF-7 cells. Mechanism II involves several proteins, including phospholipase C, protein kinase C, the type 1 inositol 1,4,5-triphosphate receptor (IP3R-1), c-Jun N-terminal kinase (JNK), and c-Jun, which have been reported to play important roles in apoptosis [2, 6, 20]. We show herein that the expression of their encoded genes was sequentially upregulated 9–24 h after MCF-7 cells were treated with the EA fraction. Moreover, expression of the cytoskeleton-related gene, *cdc42* [3], and actin-related protein 2 (ARPC2) [16] was suppressed during the early stage of

EA treatment (3–6 h after treatment). These observations may be correlated to alterations in shape and culture of EA-treated MCF-7 cells. Further biochemical and cellular biological experiments are necessary to confirm operation of the mechanism II signaling pathway in these test cells.

In conclusion, we demonstrate in this study that the EA fraction of *A. formosanus* extract triggers apoptosis in MCF-7 cells. We also tested the anti-MCF-7 cell proliferation effect of six major compounds isolated from the EA fraction, namely *α*-amyrin *trans-p*-hydroxy cinamate (2), isorhamnetin (4), kinsenoside (5), caffeic acid, quercetin, and rutin. However, none of these constituent compounds, alone or in combination, showed significant anti-MCF-7 cell proliferation as compared to the EA fraction. Obviously, we cannot rule out that untested minor components might account for the observed effect. Alternatively, the detected bioactivity of the EA fraction against MCF-7 cells might be combinational or synergistic, manifested by a group of cross-interacting phytochemicals present in the EA fraction, resulting in a relatively complex mode of action. This hypothesis is based on repeated observations and experiences of many researchers working in phytochemistry and herbal medicine. They have observed many cases of an isolated single major compound from a herbal extract which does not possess bioactivity similar to that detected in partially fractionated plant extracts. Furthermore, synergistic or cross-talk effects are now quite familiar to molecular biologists, as revealed by the large volume of findings from DNA microarray gene expression profiling and proteomic studies. We recently reported a case relevant to the present study in which a medicinal herb extract and a single-compound drug conferred similar complex pharmacogenomic activities in MCF-7 cells [28]. Therefore, many researchers acknowledge that the bioactivity of a herbal extract may not be solely dependent on the action of a single compound. We show in this study that various bioactivities detected from the partially purified (EA) fraction of the medicinal plant *A. formosanus* can in fact be highly specific as demonstrated by a series of biochemical and microarray analyses. The consistency and reproducibility of the anti-MCF-7 cell bioactivity of the EA fraction were repeatedly confirmed by qualitative and quantitative determinations of the metabolite profile and index compounds in the EA fraction. Therefore we suggest that our results provide useful scientific evidence to support that *A. formosanus* extract, a folk medicine historically used for cancer treatment, exhibits antitumor cell activities. Previously, we have also reported that the

EA fraction of *A. formosanus* exhibits significant antioxidant activity [24]. Taken together, this study suggests that the EA fraction of the *A. formosanus* extract merits further investigation as a potential cancer chemopreventive agent.

## Acknowledgments

This study was supported in part by grant NSC 91-2317-B-001-008 from the National Science and Technology Program for Agricultural Biotechnology and an institutional grant from Academia Sinica, Taipei, Taiwan, ROC.

## References

- 1 Ali M, Heaton A, Lench D. Triterpene esters from Australian *acacia*. *J Nat Prod* 60:1150–1156;1997.
- 2 Brodie C, Blumberg PM. Regulation of cell apoptosis by protein kinase C delta. *Apoptosis* 8:19–27;2003.
- 3 Brunner D. How to grab a microtubule on the move. *Dev Cell* 3:2–4;2002.
- 4 Celis JE, Kruhøffer M, Gromova I, Frederiksen C, Østergaard M, Thykjaer T, et al. Gene expression profiling: monitoring transcription and translation products using DNA microarrays and proteomics. *FEBS Lett* 481:2–16; 2000.
- 5 Chen M, Wang J. Initiator caspases in apoptosis signaling pathways. *Apoptosis* 7:313–319; 2002.
- 6 Chinnaiyan AM, Dixit VM. The cell-death machine. *Curr Biol* 6:555–562;1996.
- 7 Cuvillier O, Nava VE, Murthy SK, Edsall LC, Levade T, Milstien S, Spiegel S. Sphingosine generation, cytochrome c release, and activation of caspase-7 in doxorubicin-induced apoptosis of MCF7 breast adenocarcinoma cells. *Cell Death Differ* 8:162–171;2001.
- 8 Duggan DJ, Bittner M, Chen Y, Meltzer P, Trent JM. Expression profiling using cDNA microarrays. *Nat Genet* 21:10–14;1999.
- 9 Fang G, Chang BS, Kim CN, Perkins C, Thompson CB, Bhalla KN. 'Loop' domain is necessary for taxol-induced mobility shift and phosphorylation of Bcl-2 as well as for inhibiting taxol-induced cytosolic accumulation of cytochrome c and apoptosis. *Cancer Res* 58: 3202–3208;1998.
- 10 Jaiswal AS, Bloom LB, Narayan S. Long-patch base excision repair of apurinic/apyrimidinic site DNA is decreased in mouse embryonic fibroblast cell lines treated with plumbagin: involvement of cyclin-dependent kinase inhibitor p21Waf-1/Cip-1. *Oncogene* 21:5912–5922; 2002.
- 11 Lau WK, Chiu SK, Ma JT, Tzeng CM. Linear amplification of catalyzed reporter deposition technology on nylon membrane microarray. *Biotechniques* 33:564–570;2002.
- 12 Lin HL, Liu TS, Huang TC, Koyama T, DeVol CE. *Flora of Taiwan*. Taipei, Epoch Publishing, 1978, vol 5, pp 874–875.
- 13 Liu ZG, Hsu H, Goeddel DV, Karin M. Dissection of TNF receptor 1 effector functions: INK activation is not linked to apoptosis while NF- $\kappa$ B activation prevents cell death. *Cell* 87:565–576;1996.
- 14 Nagata S. Apoptosis by death factor. *Cell* 88: 355–365;1997.
- 15 Naujokat C, Sezer O, Possinger K. Tumor necrosis factor- $\alpha$  and interferon- $\gamma$  induce expression of functional Fas ligand on HT29 and MCF7 adenocarcinoma cells. *Biochem Biophys Res Commun* 264:813–819;1999.
- 16 Robinson RC, Turbedsky K, Kaiser DA, Marchand JB, Higgs HN, Choe S, et al. Crystal structure of Arp2/3 complex. *Science* 294: 1679–1684;2001.
- 17 Salvessen GS, Dixit VM. Caspase activation: the induced-proximity model. *Proc Natl Acad Sci USA* 96:10964–10967;1999.
- 18 Seufferlein T, Rozengurt E. Sphingosylphosphorylcholine activation of mitogen-activated protein kinase in Swiss 3T3 cells requires protein kinase C and a pertussis toxin-sensitive G protein. *J Biol Chem* 270:24334–24342;1995.
- 19 Tang D, Lahti JM, Kidd VJ. Caspase-8 activation and Bid cleavage contribute to MCF7 cellular execution in a caspase-3-dependent manner during staurosporine-mediated apoptosis. *J Biol Chem* 275:9303–9307;2000.
- 20 Thompson CB. Apoptosis in the pathogenesis and treatment of disease. *Science* 267:1456–1462;1995.
- 21 Thomposon HJ, Jiang C, Lu J, Mehta RG, Piazza GA, Paranka NS. Sulfone metabolite of sulindac inhibits mammary carcinogenesis. *Cancer Res* 57:267–271;1997.
- 22 Tian Q, Taupin JL, Elledge S, Robertson M, Anderson P. Fas-activated serine/threonine kinase (FAST) phosphorylates TIA-1 during Fas-mediated apoptosis. *J Exp Med* 182:865–874; 1995.
- 23 Verma, SP, Goldin BR. Copper modulates activities of genistein, nitric oxide, and curcumin in breast tumor cells. *Biochem Biophys Res Commun* 310:104–108;2003.
- 24 Wang SY, Kuo YH, Chang HN, Kang PL, Tsay HS, Lin KF, et al. Profiling and characterization antioxidant activities in *Anoectochilus formosanus* Hayata. *J Agric Food Chem* 5:1859–1865;2002.
- 25 Wang TH, Wang HS, Soong YK. Paclitaxel-induced cell death – where the cell cycle and apoptosis come together. *Cancer* 88:2619–2628;2000.
- 26 Woo JH, Lim YH, Choi YJ, Kim DG, Lee KS, Bae JH, Min DS, Chang JS, Jeong YJ, Lee YH, Park JW, Kwon TK. Molecular mechanisms of curcumin-induced cytotoxicity: induction of apoptosis through generation of reactive oxygen species, down-regulation of Bcl-X<sub>L</sub> and IAP, the release of cytochrome c and inhibition of Akt. *Carcinogenesis* 24:1199–1208;2003.
- 27 Yang J, Liu X, Bhalla K, Naekyung K, Ibrado AM, Cai J. Prevention of apoptosis by Bcl-2: release of cytochrome c from mitochondria blocked. *Science* 275:1129–1132;1997.
- 28 Yang NS, Shyur LF, Chen CH, Wang SY, Tzeng CM. Medicinal herb extract and a single-compound drug confer similar complex pharmacogenomic activities in MCF-7 cells. *J Biomed Sci* 11:418–422; 2004.
- 29 Yang X, Chang HY, Baltimore D. Autoproteolytic activation of pro-caspases by oligomerization. *Mol Cell* 1:319–325; 1998.